

# Theory of the waterfall phenomenon in cuprate superconductors

D. Katagiri<sup>1</sup>, K. Seki<sup>1</sup>, R. Eder<sup>1,2</sup> and Y. Ohta<sup>1</sup>

<sup>1</sup>*Department of Physics, Chiba University, Chiba 263-8522, Japan*

<sup>2</sup>*Karlsruhe Institut of Technology, Institut für Festkörperphysik, 76021 Karlsruhe, Germany*

(Dated: November 20, 2018)

Based on exact diagonalization and variational cluster approximation calculations we study the relationship between charge transfer models and the corresponding single band Hubbard models. We present an explanation for the waterfall phenomenon observed in angle resolved photoemission spectroscopy (ARPES) on cuprate superconductors. The phenomenon is due to the destructive interference between the phases of the O2p orbitals belonging to a given Zhang-Rice singlet and the Bloch phases of the photohole which occurs in certain regions of  $\mathbf{k}$ -space. It therefore may be viewed as a direct experimental visualisation of the Zhang-Rice construction of an effective single band model for the CuO<sub>2</sub> plane.

PACS numbers: 74.72.-h,79.60.-i,71.10.Fd

## I. INTRODUCTION

The 'waterfall phenomenon' observed in angle resolved photoemission spectroscopy on cuprate superconductors has attracted some attention. This phrase summarizes the following phenomenology [1–13]: for photon energies around 20 eV, where photoholes are created predominantly in O2p states[14], a 'quasiparticle band' can be seen dispersing away from the Fermi energy as  $\Gamma$  is approached but then - along the (1, 1) direction roughly at  $(\frac{\pi}{4}, \frac{\pi}{4})$  - rapidly loses intensity and cannot be resolved anymore. Instead there is a 'band' of weak intensity which seems to drop almost vertically in  $\mathbf{k}$  space towards higher binding energy, thus creating the impression of a kink in the quasiparticle band. Up to binding energies of  $\approx 1.0$  eV there is a 'black region' around the  $\Gamma$ -point with no spectral weight at all. Finally, at binding energies of around 1.0 eV the 'waterfall' seems to merge with one or several bands of high intensity, which often correspond very well to bands predicted by LDA calculations.

In experiments with photon energies  $\approx 100$ eV (where an appreciable fraction of the photoholes is created in Cu3d states[14]) and when the spectra are taken in higher Brillouin zones[7, 10], however, the low energy quasiparticle band can be resolved all the way to  $\Gamma$  and shows no indication of a kink. This band therefore undoubtedly exists and has no kink so that the only possible explanation for the 'black region' and the apparent kink seen at low photon energies are matrix element effects. This conclusion has in fact been reached by Inosov *et al.* on the basis of their experimental data[7, 10]. A very similar conclusion was also reached by Zhang *et al.*[13] who showed that the kink in the quasiparticle band appears only in the second derivative of the momentum distribution curves but is absent in the second derivative of the energy distribution curves which shows a smooth quasiparticle band instead. They concluded that the kink is not an intrinsic band dispersion.

Some support for this point of view comes from the fact that the waterfall phenomenon is observed over the whole doping range, from the antiferromagnetic insulator to the

Fermi-liquid-like overdoped compounds, so that it is obviously unrelated to any special features of the electronic structure. Moreover, the spectrum of a hole in an antiferromagnetic insulator is one of the very few reasonably well-understood problems in connection with cuprate superconductors. For this special problem good agreement between experiment[15, 16], various approximate calculations[17–24], and exact diagonalization of small clusters[25–28] has been found and no theory for hole motion in an antiferromagnet predicts a kink in the quasiparticle band. Here in particular the work of Leung and Gooding[27] should be mentioned who studied the spectral function for a single hole in a 32-site cluster by exact diagonalization and found a well-defined and smooth quasiparticle band in excellent agreement with the results of the self-consistent Born approximation[44, 45]. Moreover, since plasmons with energies below the charge transfer gap are not expected in the insulating compound and since the coupling to spin excitations is obviously described very well by the self-consistent Born approximation, a hypothetic Bosonic mode can be almost certainly ruled out as an explanation of the waterfall phenomenon in the undoped compounds and, due to the near-independence of the phenomenon on the doping level, also for the entire doping range.

One type of matrix-element effect which partly explains the nonobservation of the quasiparticle band at  $\Gamma$  has been discussed by Ronning *et al.*[1]. At the  $\Gamma$ -point in the first Brillouin zone the photoelectrons are emitted exactly perpendicular to the CuO<sub>2</sub> plane which we take as the  $(x-y)$ -plane of the coordinate system. In this situation - and if we neglect small deviations from this symmetry in the actual crystal structure - the experimental setup has  $C_{4v}$  symmetry. The expression for the photocurrent[39] involves the dipole matrix element  $\langle f|\mathbf{A} \cdot \mathbf{p}|i\rangle$ , where  $\mathbf{A}$  is the vector potential of the incoming light,  $\mathbf{p}$  is the momentum operator,  $|i\rangle$  the initial and  $|f\rangle$  the final state. The state  $|f\rangle$  differs from  $|i\rangle$  by

a) the presence of an electron in the so-called LEED state, which far from the surface evolves into a plane wave  $\propto e^{ikz}$  and hence transforms according to the iden-

tical representation

b) by the presence of a hole with momentum  $(0, 0)$  in a Zhang-Rice singlet. Since the Zhang-Rice singlet has a  $\text{Cu}3d_{x^2-y^2}$  orbital as its 'nucleus'[40] it has the same symmetry.

It follows that  $|f\rangle$  and  $|i\rangle$  have the same parity under reflection in the  $x - y$  plane so that the dipole matrix element is zero if  $\mathbf{A}$  is in the  $\text{CuO}_2$  plane. On the other hand  $|f\rangle$  and  $|i\rangle$  acquire a relative minus-sign under a rotation by  $\frac{\pi}{2}$  around the  $z$ -axis so that the dipole matrix element is zero as well if  $\mathbf{A}$  is perpendicular to the  $\text{CuO}_2$  plane. This means that it is impossible to observe a state with the character of a Zhang-Rice singlet at  $\Gamma$  in normal emission. As Ronning *et al.* pointed out, however, this argument cannot explain the nonobservation of the quasiparticle band at  $\Gamma$  in higher Brillouin zones, where the photoelectrons are no longer emitted in the direction perpendicular to the surface.

Moreover, a similar effect has been observed in ARPES studies of the compound  $\text{SrCuO}_2$  which contains  $\text{CuO}$  chains. With a photon energy of  $22.4 \text{ eV}$  and polarization parallel to the chains - which generates holes in  $\sigma$ -bonding  $\text{O}2p$  orbital - there is no intensity at  $k = 0$ [29]. If the photon energy is increased to  $100 \text{ eV}$ , however, the spinon-band around  $k = 0$  can indeed be resolved[30]. This behaviour is similar to the waterfall effect but in this compound the  $\text{CuO}_2$  plaquettes are perpendicular to the surface of the crystal. We conclude that there must be a second mechanism for the extinction of spectral weight around  $\Gamma$  in both, the one and two dimensional systems. An explanation of the waterfall phenomenon has been given by Basak *et al.*[31]. These authors first showed that the waterfall phenomenon cannot be reproduced by a calculation of ARPES spectra from LDA band structures and eigenfunctions alone, a procedure which has otherwise been found to be highly successful in describing ARPES spectra of cuprate superconductors[32, 33]. Instead, these authors obtained good agreement with experiment by additionally introducing a self-energy which describes the coupling to a Bosonic mode. The basic mechanism for the waterfall and the variation of the ARPES spectra with photon energy then is bilayer splitting which is enhanced by the coupling to the Bosonic mode, in particular the vertical part of the waterfall turns out to be the strongly renormalized bonding combination of the two single-layer wave functions. This model reproduces the strong changes of ARPES spectra with photon energy  $h\nu$  in the range  $60 \text{ eV} \rightarrow 80 \text{ eV}$  as observed by Inosov *et al.*[7, 10] quite well. On the other hand, Inosov *et al.* gave a different explanation for this variation, namely the rapid variation of the  $\text{Cu}3d$  photoemission intensity at the  $\text{Cu } 3p \rightarrow 3d$  absorption threshold at  $75 \text{ eV}$ . Since the strong variation of photoemission spectra at the  $3p \rightarrow 3d$  threshold is well established for  $3d$  transition metal oxides[34] this appears a plausible explanation.

There have been attempts to reproduce a kink in the band structure within the framework of a single-band Hubbard or t-J model[35–37]. The high-intensity bands



FIG. 1: (Color online) Possible realization of the model (1).

observed near  $\Gamma$  at binding energies of  $\approx 1.0 \text{ eV}$  thereby are identified with high energy features observed previously in exact diagonalization[25–27] or Quantum Monte-Carlo[38] studies for such models.

In the present manuscript we take the point of view that the waterfall phenomenon is a pure matrix-element effect, as pointed out by Inosov *et al.*[7, 10] and Zhang *et al.*[13]. Thereby the crucial point is the nature of the low-energy hole states as Zhang-Rice singlets. Since the phases of the  $\text{O}2p$  hole 'within' a Zhang-Rice singlet correspond to momentum  $(\pi, \pi)$ [40] there is perfect destructive interference with the phases of a p-like photohole with momentum  $(2n\pi, 2m\pi)$  with  $n$  and  $m$  integer. The quasiparticle band at  $\Gamma$  therefore can be observed only at photon energies where the cross section for hole creation in  $d$ -orbitals is large - because the destructive interference occurs only for  $\text{O}2p$ -photoholes - and in higher Brillouin zones where the argument by Ronning *et al.*[1] does not apply.

In section II we will discuss exact diagonalization results for a 1-dimensional charge transfer model. In section III we discuss the spectra of a 2-dimensional charge transfer model by the variational cluster approximation (VCA). In section IV we discuss the experimental relevance of the binding energy of the Zhang-Rice singlet and section V gives summary and conclusions.

## II. ONE DIMENSIONAL MODEL

We study a 1-dimensional (1D) charge transfer model by exact diagonalization. We choose a 1D model because we need at least a two-band model and the largest cluster of a two-band model we can study in 2D contains 4  $\text{Cu}$ -ions, so that we have virtually no  $\mathbf{k}$ -resolution. As will be seen below, however, a very simple 1D model is sufficient to reproduce the key features of the waterfall phenomenon. To be more precise, the Hamiltonian reads

$$H = t \sum_{i,\sigma} \left[ d_{i,\sigma}^\dagger (p_{i+\frac{1}{2},\sigma} - p_{i-\frac{1}{2},\sigma}) + H.c. \right] + \Delta \sum_i n_{d,i} + U \sum_i n_{d,i,\uparrow} n_{d,i,\downarrow} \quad (1)$$

where  $d_{i,\sigma}^\dagger$  ( $p_{j,\sigma}^\dagger$ ) creates a hole in a  $d$ -like orbital at site  $i$  ( $p$ -like orbital at site  $j$ ). We choose  $t$  as the unit of energy and use the values  $\Delta = -4$  and  $U = 8$  throughout. The crucial feature of the model is that - as in the case for the  $\text{CuO}_2$  plane- the  $d - p$  hybridization integral has an alternating sign. A schematic representation of the model is shown in Figure 1. Figure 2 shows the single particle

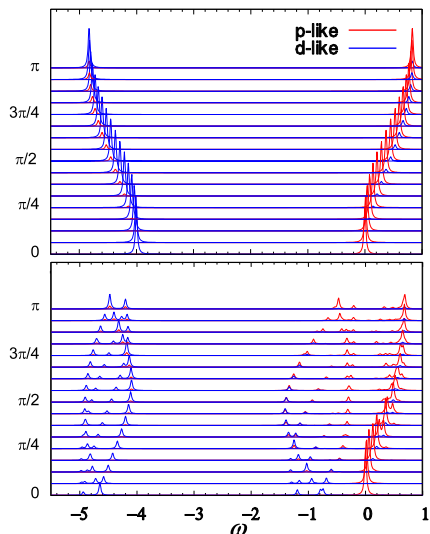


FIG. 2: (Color online) Single particle spectral function for the model (1) for the half-filled system (8 holes in 8 unit cells). The Figure combines spectra calculated with different boundary conditions to give an impression of larger systems. The right part of the spectra corresponds to hole creation (i.e. photoemission) the left part to hole annihilation (inverse photoemission). The upper figure shows the spectra for  $U = 0$ , the lower one the spectra for  $U = 8$ .

spectral function for the noninteracting case  $U = 0$  and for the strongly correlated case  $U = 8$ . These are defined as

$$A_d(\mathbf{k}, \omega) = -\frac{1}{\pi} \Im G_{dd}(\mathbf{k}, \omega + i\eta) \quad (2)$$

where  $G_{dd}$  is the  $d$ -like diagonal element of the  $2 \times 2$  single-particle Green's function (and analogously for  $A_p(\mathbf{k}, \omega)$ ). The Lorentzian broadening  $\eta = 0.1$ . In the noninteracting case there are two bands, one with predominant  $p$ -character and one with predominant  $d$ -character. Since the matrix element of the  $p-d$  hybridization is  $\propto \sin(\frac{k}{2})$  there is no  $p-d$  hybridization for  $k = 0$  and the states have pure  $p$ - or  $d$ -character. Also, the energy of the  $p$ -like peak agrees exactly with that of the  $p$ -orbital, i.e. 0.

Surprisingly the  $p$ -like band can be identified also in the strongly correlated case, particularly so near  $k = 0$ . The reason is that the  $p$ -like Bloch state with  $k = 0$  does not mix with the  $d$ -like Bloch state due to parity so that a hole created in this state is unaffected by the Coulomb repulsion on the  $d$ -sites. Accordingly, the energy of this peak still is 0. This state is analogous to the '1 eV-peaks' in the real cuprate materials[42]. Near  $k = 0$  the mixing still is small so that  $U$  is effectively only a weak perturbation.

On the other hand the upper band of predominant  $d$ -character disappears completely and is replaced by a spectrum which is very similar to that of a 1D single-band Hubbard model. This can be seen in Figure 3 which

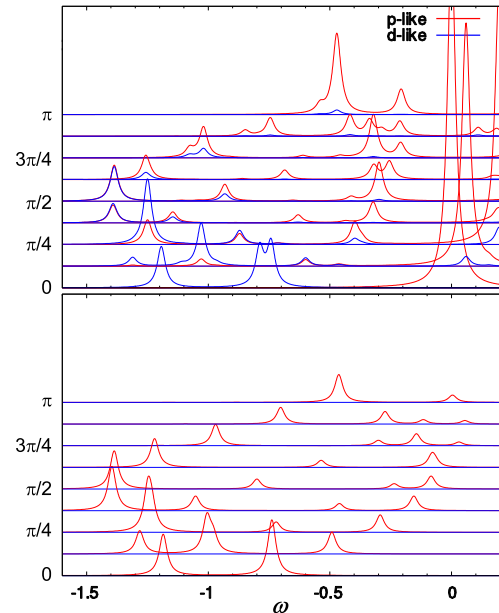


FIG. 3: (Color online) Top: Closeup of the hole addition part of the spectrum in Figure 2. Bottom: Photoemission spectrum for a half-filled single-band Hubbard chain with 8 sites and  $U'/t' = 10.8$  and  $t' = 0.335 t$ . The single-band spectrum has been turned 'upside down' to be compatible with the hole picture and shifted by  $0.87t$ . The figure combines spectra calculated with periodic and antiperiodic boundary conditions.

shows a close-up of the low energy region of the photoemission (i.e. hole addition) spectrum and compares this to the photoemission spectrum of a single-band Hubbard model. It turns out that for the above values of  $t$ ,  $U$  and  $\Delta$  a very good match can be obtained by choosing the parameters of the single-band Hubbard model to be  $U'/t' = 10.8$  and  $t' = 0.335 t$ . There is a rather obvious one-to-one correspondence between the peaks, the different 'holon bands' characteristic for the spectra of finite clusters of the one-dimensional Hubbard or t-J model[43] can be identified in both spectra. The main difference occurs at energies  $E$  between  $-0.5$  and  $0$ . This is most likely the consequence of mixing and level repulsion between the single-band Hubbard-like bands and the free-electron-like  $p$  band. Moreover one can see a splitting of some of the peaks in the two-band model.

The full interacting spectrum therefore can be modelled well by superposing the lower noninteracting  $p$  band and a single band Hubbard spectrum. This indicates that the Zhang-Rice construction[40] for reduction of the low-energy sector of the two-band model to a single band model also works well for this 1D model. On the other hand, for higher energies the 2-band model has additional states which correspond to the non-bonding combination of  $p$ -orbitals.

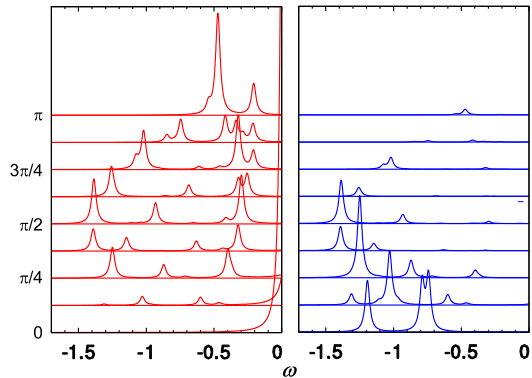


FIG. 4: (Color online) Closeup of the hole addition part of the spectrum in Figure 2. The left panel shows the  $p$ -like spectrum, the right panel the  $d$ -like spectrum.

Figure 4 shows the photoemission spectrum of the two-band model split into its  $p$ - and  $d$ -component. This demonstrates that the key features[7, 10] of the waterfall phenomenon can be seen already in this simple 1D model: Near  $\Gamma$  there is no  $p$ -like intensity in the single-band Hubbard-like states, instead all  $p$ -like intensity resides in the free-electron-like band (this is the huge peak at  $E = 0$ ). The  $p$ -like intensity alone therefore shows the black region around  $k = 0$  and a 'high-energy-kink' whereby the vertical part of the waterfall is due to the incoherent continuum of the single-particle spectrum of the single-band Hubbard model. In the  $d$ -like spectrum on the other hand the quasiparticle band can be followed right up to the  $\Gamma$ -point. Already this simple model therefore reproduces the key features of the waterfall phenomenon and the photon energy dependence of the spectra: the waterfall occurs in the first Brillouin zone for all photon energies and in higher Brillouin zones for photon energies where the cross section for Cu3d is small.

To understand the extinction of  $p$ -like weight around  $\Gamma$  we repeat the Zhang-Rice construction[40] and consider a single plaquette - which in the 1D model consists of the  $d$ -orbital and its two nearest neighbor  $p$ -orbitals - at the  $d$ -site  $\mathbf{R}_i$ . For one hole, the ground state reads

$$\begin{aligned} |\Psi_{0,\sigma}^1\rangle &= (u_1 p_{i,-,\sigma}^\dagger + v_1 d_{i\sigma}^\dagger)|0\rangle \\ p_{i,-,\sigma}^\dagger &= \frac{1}{\sqrt{2}}(p_{i+\frac{1}{2},\sigma}^\dagger - p_{i-\frac{1}{2},\sigma}^\dagger). \end{aligned} \quad (3)$$

The coefficients  $(u_1, v_1)$  are the GS eigenvector of the matrix

$$H^{1h} = \begin{pmatrix} 0 & \sqrt{2}t \\ \sqrt{2}t & \Delta \end{pmatrix}. \quad (4)$$

The singlet ground state - i.e. the analogue of a Zhang-Rice singlet in the 1D model - of two holes is

$$\begin{aligned} |\Psi_0^2\rangle &= (u_2 p_{-,\uparrow}^\dagger p_{-,\downarrow}^\dagger + \frac{v_2}{\sqrt{2}} (d_{\uparrow}^\dagger p_{-,\downarrow}^\dagger + p_{-,\uparrow}^\dagger d_{\downarrow}^\dagger) \\ &\quad + w_2 d_{\uparrow}^\dagger d_{\downarrow}^\dagger)|0\rangle \end{aligned}$$

and the coefficients  $(u_2, v_2, w_2)$  are the GS eigenvector of the matrix

$$H^{2h} = \begin{pmatrix} 0 & 2t & 0 \\ 2t & \Delta & 2t \\ 0 & 2t & 2\Delta + U \end{pmatrix}. \quad (5)$$

In the corresponding single-band model, the state  $|\Psi_{0,\sigma}^1\rangle$  corresponds to the site  $i$  being occupied by a spin- $\sigma$  electron, whereas  $|\Psi_0^2\rangle$  corresponds to a hole at site  $i$ . The matrix element of the electron annihilation operator  $c_{\mathbf{k},\uparrow}$  between these states is  $e^{i\mathbf{k}\cdot\mathbf{R}_i}$ . On the other hand, the matrix elements of the operators  $p_{\mathbf{k},\uparrow}$  and  $d_{\mathbf{k},\uparrow}$  are

$$\begin{aligned} m_p(k) &= e^{i\mathbf{k}\cdot\mathbf{R}_i} \sqrt{2} i \sin\left(\frac{k}{2}\right) (u_1 u_2 + \frac{1}{\sqrt{2}} v_1 v_2) \\ m_d(k) &= e^{i\mathbf{k}\cdot\mathbf{R}_i} \left(\frac{1}{\sqrt{2}} u_1 v_2 + v_1 w_2\right). \end{aligned} \quad (6)$$

The crucial term here is the factor of  $i \sin(\frac{k}{2})$  which arises from the overlap of the  $p$ -like Bloch state with momentum  $k$  and the bonding combination  $p_{i,-,\sigma}^\dagger$ . In addition, we have to take into account a shift in energy of  $\epsilon = E_0^{1h} - E_0^{2h}$ . This corresponds to the binding energy of the ZRS and has no counterpart in the single-band model. In simplest terms, we would therefore expect that the photoemission part of single particle spectral functions of the two-band model can be obtained from that of the single band model by

$$A_{p,d}(k, \omega) = |m_{p,d}(k)|^2 A(k, \omega + \epsilon). \quad (7)$$

In this expression several simplifications have been made: the ZRS is assumed to extend only over one plaquette, which is probably not correct. This implies that processes where a ZRS in a plaquette around site  $i$  is generated by actually creating a hole in a neighboring unit cell are neglected. Moreover the problem of the overlap of Zhang-Rice singlets in neighboring cells[40] is not taken into account either.

The energy shift  $\epsilon$  which is necessary to match the two spectra in Figure 3 is found to be  $0.87 t$  - the estimate obtained from the eigenvalues  $E_0^{1h}$  and  $E_0^{2h}$  is  $1.04 t$ , i.e. reasonably close. Figure 5 shows the spectra obtained from equation (7) compared to the actual spectra of the two-band model. The numerical values of the prefactors are  $u_1 u_2 + \frac{1}{\sqrt{2}} v_1 v_2 = 0.70$  and  $\frac{1}{\sqrt{2}} u_1 v_2 + v_1 w_2 = 0.50$ . While the agreement is not really perfect, the qualitative trends are reproduced well, particularly so near  $k = 0$  where the hybridization with the  $p$ -like band is weak. The main differences occur for larger  $k$ -values and may also be due to the fact that the ZRS is not restricted to

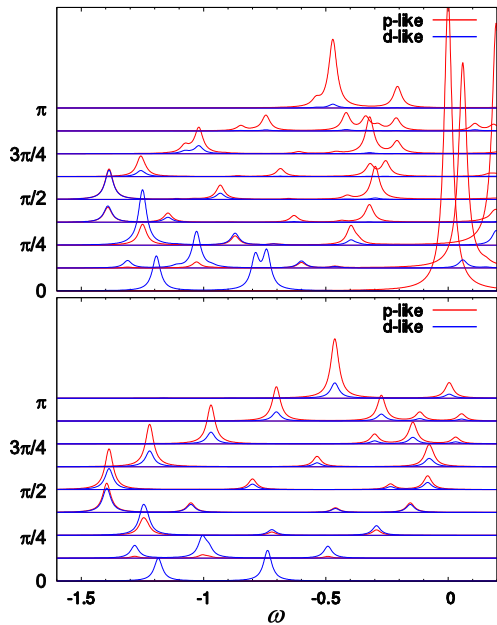


FIG. 5: (Color online) Closeup of the photoemission spectrum in Figure 2 (Top) compared to the spectra of a single-band Hubbard model corrected according to (7) (Bottom). The energy shift  $\epsilon$  is  $0.84 t$  rather than  $1.04 t$  as would be obtained from the single-plaquette calculation.

one plaquette and also the hybridization with the  $p$ -like band which is absent in the single-band Hubbard model. On the other hand, given the simplicity of the procedure for converting the single-band spectra into two-band spectra this not so bad and qualitatively explains the extinction of  $p$ -like intensity around  $\Gamma$  at least qualitatively: this is due to the factor of  $\sin(\frac{k}{2})$  in the matrix element  $m_p$ , which describes the destructive interference between the phase factors of the two  $p$ -orbitals in the bonding combination  $p_{-,\sigma}^\dagger$  and in the electron operator  $p_{k,\sigma}^\dagger$ . This is in turn the consequence of the oscillating sign of the hopping integral in (1) so that the same mechanism should also be effective in the 2D  $\text{CuO}_2$ -plane.

The exact diagonalization results then can be summarized as follows: The oscillating sign of the  $d-p$  hybridization induces an oscillating sign also in the bonding combination of  $p$ -orbitals around a given  $d$ -site. The phase of the  $p$ -orbitals in the bonding combination therefore 'locally' corresponds to a momentum of  $\pi$ . It follows that around  $k = 2n\pi$  there is destructive interference between the phases of the bonding combination and the phases of the photohole, and it is not possible to couple to the ZRS by hole creation in  $p$ -orbitals. The ZRS-part of the spectrum thus becomes extinct in the  $p$ -like spectrum, whereas no such extinction occurs in the  $d$ -like spectrum. To conclude this section we note that none of the above considerations is limited to half-filling. Figure 6 compares the spectra for the 2-band model and the

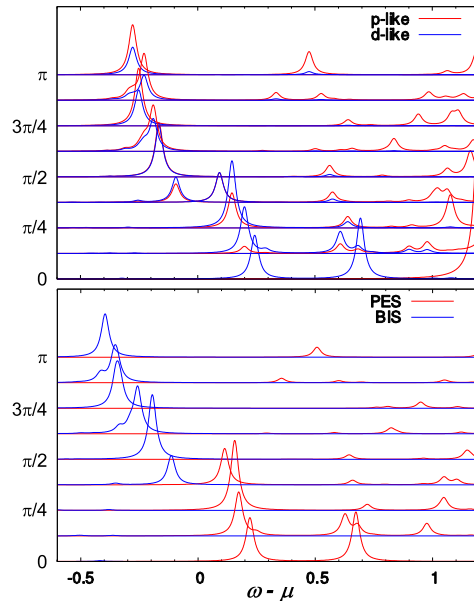


FIG. 6: (Color online) Low energy photoemission spectrum of the hole-doped two-band model compared to the spectrum of the corresponding single-band model. In this figure, the chemical potential is the zero if energy.

single-band model in the hole-doped case, that means at a hole density of 1.25. Thereby all parameters are the same as in Figure 4. Again, a very good correspondence between the two models exists and again the extinction of  $p$ -like weight around  $k = 0$  can be clearly seen.

### III. 2 DIMENSIONAL MODEL

We now apply the picture gained from the analysis of the one-dimensional two-band model to obtain approximate ARPES spectra for the 2D  $\text{CuO}_2$ -plane. Since it is not possible to compute the spectra of a 2D three-band model larger than  $2 \times 2$  unit cells by exact diagonalization we switch to the variational cluster approximation (VCA)[49, 50, 52] to compute at least approximate spectra. The VCA uses the fact[51] that the grand canonical potential of an interacting Fermi system can be expressed as a functional of the self-energy  $\Sigma(\omega)$  and is stationary with respect to variations of  $\Sigma(\omega)$  at the exact self-energy. The VCA then uses finite clusters - the so-called reference system - to numerically generate 'trial self energies' for an infinite system. This is described in detail in the literature[49, 50, 52] and has turned out to be a very successful method to discuss the single-particle spectral functions of correlated electron systems. We use this method to calculate spectra for the three-band Hub-

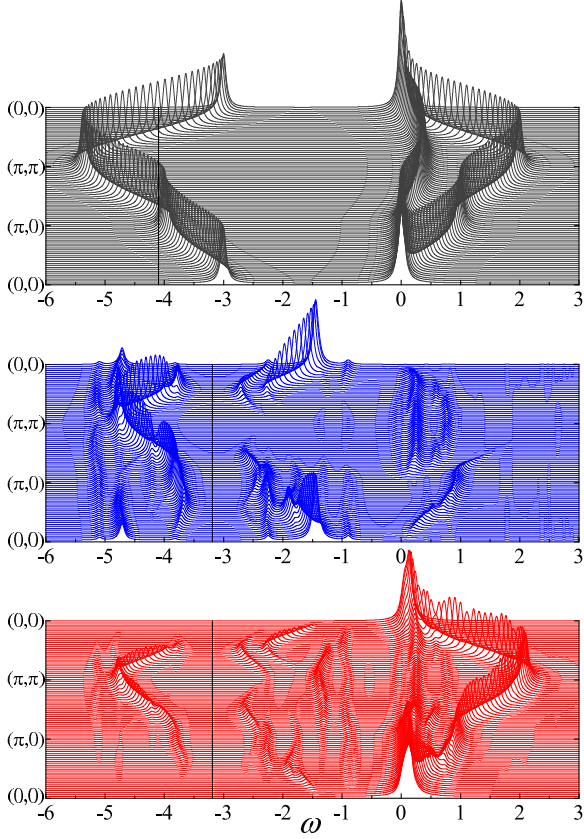


FIG. 7: (Color online) Top: Sum of  $p$ -like and  $d$ -like spectrum for the three-band model (8) with  $U = 0$ . Center:  $d$ -like spectrum for  $U = 8$  as obtained by the VCA. The spectrum has been multiplied by 2.5. Bottom:  $p$ -like weight for  $U = 8$ . The spectra are computed for half-filling, that means 1 hole/unit cell, the black line denotes the respective chemical potential.

bard model

$$\begin{aligned}
H = & 2t_{pd} \sum_{i \in L_d, \sigma} \left( d_{i,\sigma}^\dagger P_{i,\sigma} + H.c \right) \\
& + 2t_{pp} \sum_{\alpha=x,y} \sum_{j \in L_\alpha, \sigma} \left( p_{\alpha,j,\sigma}^\dagger Y_{\alpha,j,\sigma} + H.c \right) \\
& - \Delta \sum_{i \in L_d} n_{d,i} + U_{dd} \sum_{i \in L_d} n_{d,i,\uparrow} n_{d,i,\downarrow} \\
& + U_{pp} \sum_{j \in L_\alpha} n_{p,j,\uparrow} n_{p,j,\downarrow}. \quad (8)
\end{aligned}$$

$L_d$  denotes the s.c. lattice of Cu3d sites,  $L_x$  and  $L_y$  the s.c. lattices of  $p_x$  and  $p_y$  sites. Moreover

$$P_{i,\sigma}^\dagger = \frac{1}{2} \left( p_{x,i-\frac{\hat{x}}{2},\sigma}^\dagger - p_{x,i+\frac{\hat{x}}{2},\sigma}^\dagger - p_{y,i-\frac{\hat{y}}{2},\sigma}^\dagger + p_{y,i+\frac{\hat{y}}{2},\sigma}^\dagger \right) \quad (9)$$

is the bonding combination of  $p$ -orbitals around the  $d$ -orbital at site  $i$  and

$$Y_{\alpha,i,\sigma}^\dagger = \frac{1}{2} \left( p_{\hat{\alpha},i+\frac{\hat{x}}{2}-\frac{\hat{y}}{2},\sigma}^\dagger - p_{\hat{\alpha},i+\frac{\hat{x}}{2}+\frac{\hat{y}}{2},\sigma}^\dagger + p_{\hat{\alpha},i-\frac{\hat{x}}{2}+\frac{\hat{y}}{2},\sigma}^\dagger - p_{\hat{\alpha},i-\frac{\hat{x}}{2}-\frac{\hat{y}}{2},\sigma}^\dagger \right) \quad (10)$$

for  $\alpha = x$  denotes the bonding combination of  $p_y$  orbitals around a given  $p_x$  orbital and vice versa for  $\alpha = y$ .  $\hat{\alpha}$  denotes the unit vector in  $\alpha$ -direction. The model is again formulated in hole language, i.e.  $d_{i,\sigma}^\dagger$  creates a hole in orbital  $i$  and  $t_{pd}, t_{pp} > 0$ . We choose  $t_{pd}$  as the unit of energy, the other parameters are  $U_{dd} = 8$ ,  $U_{pp} = 3$ ,  $\Delta = 3$ ,  $t_{pp} = 0.5$ . We study this model by the VCA, using a cluster with  $2 \times 2$  unit cells (i.e. a square shaped  $\text{Cu}_4\text{O}_8$  cluster) with 4 holes (corresponding to 'half filling') as the reference system for creating trial self-energies. Some results obtained in this way for this model have previously been published by Arrigoni *et al.*[53]. Figure 7 shows the total spectral weight for the case  $U = 0$  as well as the  $p$ -like and  $d$ -like spectral weight for the interacting case,  $U = 8$ . The  $p$ -like spectral weight now is defined as the sum of the two  $p$ -like diagonal elements of the total  $3 \times 3$  spectral weight matrix.

In the noninteracting case,  $U = 0$ , there are three bands. Switching on the Coulomb repulsion has a very similar effect as for the 1D model: The two upper (in hole language) bands with predominant  $p$  character remain essentially unchanged, whereas the partly filled band of predominant  $d$ -character is split into an upper and a lower Hubbard band. Comparing the  $p$  and  $d$  spectra in the energy range  $0 \rightarrow 2t_{pd}$  the same extinction of  $p$ -like spectral weight around  $(0,0)$  can be seen i.e. exactly the same behaviour as in the 1D model.

By analogy with the 1D case we assume that the reason for the extinction of  $p$ -like weight again is the matrix element between a plane wave of  $p$  holes and the bonding combination (9). We again consider a single-plaquette problem. For later reference we include a Coulomb repulsion  $U_{pd}$  between  $p$  and  $d$ -holes on neighboring sites which is set equal to zero for the time being. The Hamilton matrices for the single and two hole plaquette problems are:

$$H^{1h} = \begin{pmatrix} -2t_{pp} & 2t_{pd} \\ 2t_{pd} & \Delta \end{pmatrix} \quad (11)$$

$$H^{2h} = \begin{pmatrix} -4t_{pp} + \frac{U_{pp}}{4} & 2\sqrt{2}t_{pd} & 0 \\ 2\sqrt{2}t_{pd} & \Delta - 2t_{pp} + U_{pd} & 2\sqrt{2}t_{pd} \\ 0 & 2\sqrt{2}t_{pd} & 2\Delta + U_{dd} \end{pmatrix}. \quad (12)$$

The  $p-p$  Coulomb repulsion  $\propto U_{pp}$  is treated in mean-field theory. The ground state eigenvectors of these matrices are again denoted by  $(u_1, v_1)$  and  $(u_2, v_2, w_2)$ .

To discuss the  $p$ -like photoemission spectrum we need the matrix element between the bonding combination (9) and a  $p$ -like Bloch wave. We write this as

$$m_p = -i \left[ m_x \sin\left(\frac{k_x}{2}\right) - m_y \sin\left(\frac{k_y}{2}\right) \right], \quad (13)$$

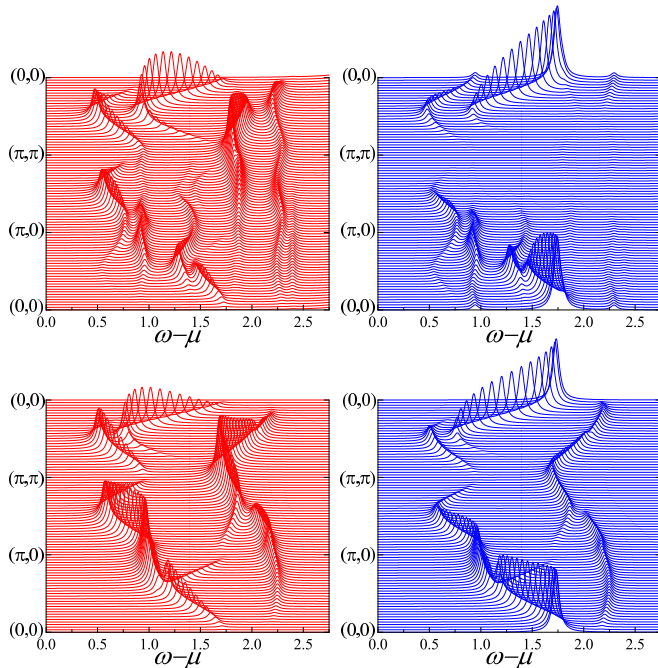


FIG. 8: (Color online) Right part:  $d$ -like spectrum of the three-band model (top) compared to the spectrum of the single band Hubbard model multiplied by 0.5 (bottom). Left part:  $p$ -like spectral weight of the three-band model multiplied by 2 (top) compared to the spectrum of the single band Hubbard model multiplied by 0.5  $f(\mathbf{k})$  in (14) (bottom).

where  $m_\alpha$  ( $\alpha \in x, y$ ) are matrix elements for hole creation in a  $p_\alpha$  orbital at the origin, which in a real experiment depend e.g. on the photon polarization and wave vector of the photoelectrons. In the present calculation  $A_p(\mathbf{k}, \omega)$  is obtained by calculating the spectra for creating holes in  $p_x$  and  $p_y$  orbitals separately and adding them - accordingly, the  $\mathbf{k}$ -dependent correction factor in (7) should be replaced by[54]

$$m_p^2(\mathbf{k}) = (u_1 u_2 + \frac{1}{\sqrt{2}} v_1 v_2)^2 f(\mathbf{k})$$

$$f(\mathbf{k}) = \sin^2\left(\frac{k_x}{2}\right) + \sin^2\left(\frac{k_y}{2}\right) \quad (14)$$

To check this we have calculated the photoemission spectrum of a the single-band Hubbard model by the VCA using again a  $2 \times 2$  cluster as reference system. We use the  $2 \times 2$  cluster as reference system in order to make the spectra of the two models as comparable as possible. By using the same reference system gaps in the VCA bands which originate from the supercell structure which is unavoidably introduced by the VCA should be more or less identical in both spectra. The parameter values of the single band model are again chosen to obtain a good match with the dispersion of the three-band model. Thereby in addition to the nearest neighbor hopping integral  $t'$  also hopping integrals  $t'_1$  between second-nearest neighbors and  $t'_2$  between third nearest neighbors were included. A good match was obtained by using  $t'/t_{pd} = 0.38$ ,  $t'_1/t' = -0.145$ ,  $t'_2/t' = 0.118$  and  $U'/t' = 10.3$ . Figure 8

compares the low energy hole addition spectrum of the three band model with the (shifted) photoemission spectrum of the single band model. The  $d$ -like spectrum of the three-band model should be roughly identical to that of the single band Hubbard model and the two spectra on the right part of the figure are indeed quite similar. There are two main differences: the weakly dispersive band at  $\approx 1.75t_{pd}$  which can be seen in the single band model is absent in the spectrum of the three-band model. This may be a consequence of hybridization with the two additional  $p$ -like bands in the three-band model. Moreover, the spectrum for the three-band model has a less smooth dispersion with additional gaps along  $(0,0) \rightarrow (\pi,0)$ . This is likely due to the lower symmetry of the three-band model: in the single band Hubbard model, the  $2 \times 2$  cluster with open boundary conditions is equivalent to a 4-site chain with periodic boundary conditions. For the two band model a similar reduction is possible, but with two  $p$  orbitals in between any two successive  $d$  orbitals. The resulting degeneracy of the ligands in the 4-site chain may give rise to the additional band splitting. The left part of the Figure compares the  $p$ -like spectrum of the three-band model and the single band model spectrum corrected by the factor  $m_p(\mathbf{k})$ . Again, the dispersion of the spectral weight along comparable bands is very similar in the two spectra. The energy shift to align the single-band and three-band spectra is  $\epsilon = 2.00 t_{pd}$ . The estimate obtained from the ground state energies of the matrices (11) and (12) is  $E_0^{1h} - E_0^{2h} = 2.238 t_{pd}$ . The error of  $\approx 10\%$  seems reasonable taking into account the various approximations made. To match the intensities of the single-band and three-band spectra in Figure 8 the single band spectra were multiplied by a factor of 0.5. The estimates for the correction factors from the single-plaquette problem are  $(u_1 u_2 + \frac{1}{\sqrt{2}} v_1 v_2)^2 = 0.56$  and  $(\frac{1}{\sqrt{2}} u_1 v_2 + v_1 w_2)^2 = 0.31$ .

To summarize the discussion so far: the low-energy hole addition spectrum of the three-band model can be obtained to reasonable approximation from an effective single-band model whereby the  $p$ -like spectrum needs to be corrected by a simple  $\mathbf{k}$ -dependent factor which originates from the interference between the phases of  $p$ -orbitals in the bonding combinations and the phases in a Bloch state with momentum  $\mathbf{k}$ . If this correction is done  $p$ -like and  $d$ -like spectra can be obtained to good approximation from the spectrum of a single band Hubbard model.

We now apply this finding to compute approximate the spectra for a  $\text{CuO}_2$  plane, but this time make use of the fact that in a single-band Hubbard model larger clusters can be used as a reference system. We again apply the VCA but this time we use a  $4 \times 4$  cluster with periodic boundary conditions as reference system. We used a cluster with 2 holes corresponding to a hole concentration of 12.5%. It is important to use as large a cluster as possible for the exact diagonalization step, because only large clusters reproduce the incoherent continua in the spectral function sufficiently well and, as will be seen

below, these incoherent continua are crucial to explain the experimentally observed spectra. Solution of a  $4 \times 4$  cluster by exact diagonalization is only possible with periodic boundary conditions, which are not customary in VCA calculations. On the other hand, we do not want to discuss the phase diagram of the Hubbard model but we mainly want to obtain the spectral function so this is justified. In fact, the spectral function obtained by the simpler cluster perturbation theory[55, 56] is almost exactly the same as the one obtained by VCA.

Having obtained an approximate spectrum for the single-band Hubbard model we again use (7) together with (14) to obtain the  $d$ -like and  $p$ -like intensity for the three-band model. This is shown in Figure 9 for momenta along the  $(1, 1)$  direction.

It can be seen that the Figure reproduces the waterfall effect quite well. In the  $d$ -like spectrum the low-energy quasiparticle band can be seen together with a broad high intensity part at more negative binding energy. Moreover there is appreciable incoherent weight around  $\mathbf{k} = (0, 0)$ . These incoherent continua are well known from exact diagonalization[25–28] and self-consistent Born calculations[44, 45] for the  $t$ -J model. Their intensity decreases with increasing distance from  $\mathbf{k} = (0, 0)$ . This decrease is due to the coupling of photoholes to spin and charge fluctuations[24]. In the  $p$ -like spectrum the factor  $m_p^2(\mathbf{k})$  in (14) creates the dark region around  $\mathbf{k} = (0, 0)$ . Accordingly, the quasiparticle band seems to disappear at  $\approx (\frac{\pi}{4}, \frac{\pi}{4})$ . Since the incoherent weight is reduced by the same factor  $m_p^2(\mathbf{k})$ , it disappears at the same momentum which creates the impression of a 'band' which has a kink at  $\approx (\frac{\pi}{4}, \frac{\pi}{4})$ . At the kink the spectral weight of the band drops sharply. Qualitatively this is exactly what is seen in the ARPES spectra which show the waterfall phenomenon. The chimney-like appearance of the spectrum is due to the fact that the  $d$ -like spectral weight can be approximated by a product:  $A_p(k, \omega) = |m_p(k)|^2 A(k, \omega + \epsilon)$ . For fixed  $\omega$  the second factor,  $A(k, \omega + \epsilon)$  decreases with  $|\mathbf{k}|$  - see the left part of Figure 9 - whereas the first factor,  $|m_p(k)|^2$  vanishes at  $\mathbf{k} = (0, 0)$  and increases with  $|\mathbf{k}|$ . Accordingly, the  $p$ -like spectral weight must go through a maximum and this maximum corresponds to the apparent vertical part of the band. For a quantitative discussion it would be necessary to take into account also the interference between hole creation in  $\text{Cu}3d_{x^2-y^2}$  and  $\text{O}2p$  orbitals. This however would necessitate to know the relative magnitude and phase of the respective dipole matrix elements and this is beyond the scope of the present paper.

#### IV. DIRECT MEASUREMENT OF THE BINDING ENERGY OF THE ZRS

Lastly we wish to point out that the energy shift  $\epsilon$  - i.e. the binding energy of the ZRS - does indeed have some relevance for the interpretation of experimental data and has in a sense been observed directly. We refer to the re-

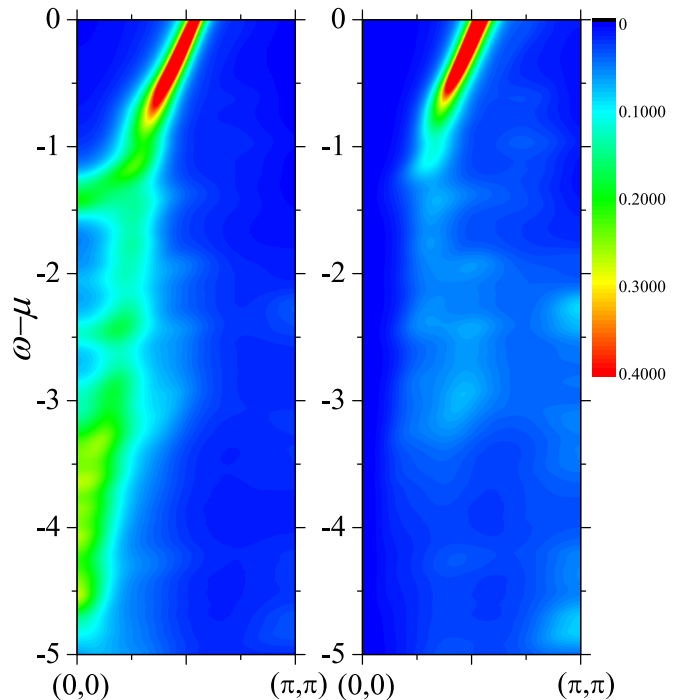


FIG. 9: (Color online) Left: Spectral function of the the single band Hubbard model with  $U = 10$ ,  $t = 1$ . Right: Spectral function of the the single band Hubbard model multiplied by  $f(\mathbf{k})$  (see (14)).

sults of Meevasana *et al.*[8]) who reported an anomalous enhancement of the noninteracting bandwidth in  $\text{Bi}2201$ . These authors pointed out that the energy difference between an assumed band bottom at  $\Gamma$  and the Fermi energy seems to be larger than the occupied bandwidth predicted by LDA calculations and concluded that there is an anomalous correlation induced band widening rather than the expected correlation narrowing.

We now estimate the position of  $\mu$  with respect to an '1eV' peak as an intrinsic reference energy and show that the Fermi energy can be obtained quite accurately from a single-band Hubbard or  $t$ -J model by consequent application of the Zhang-Rice construction[40]. To begin with, Meevasana *et al.* observed a band at  $\Gamma$  with downward curvature and a binding energy of  $\approx -1$  eV relative to the Fermi level at  $\Gamma$  (this is the band labelled B in Figure 1 of Ref. [8]). The authors point out that this is an umklapp of a band at the  $Y$ -point, or  $(\pi, \pi)$  in a simple cubic 2D model. This is therefore probably the same state as shown in Fig. 3(c) of Ref. [42], i.e. a state composed of  $\text{O}2p\pi$  orbitals which right at  $(\pi, \pi)$  has zero hybridization with any of the correlated  $\text{Cu}3d$  orbitals. Inspection of Fig. 3(c) of Ref. [42] shows that the energy of an *electron* in this state at  $(\pi, \pi)$  - and accordingly its umklapp at  $\Gamma$  - is  $E_1 = \epsilon_p + 4t_{pp}$  where  $\epsilon_p$  is the orbital energy for  $\text{O}2p$  electrons. Since this is a single-particle-like state, the corresponding binding energy in the photoemission spectrum is  $E_0^N - E_\nu^{N-1} = E_1$ . Next, we consider the Fermi energy. The largest part of



the energy shift thereby is the binding energy of the ZRS,  $\epsilon$ , which was discussed above. In the matrices (11) and (12) the energy of a hole in an O2p orbital, i.e.  $-\epsilon_p$ , was chosen as the zero of energy so that we have to change  $\epsilon \rightarrow \epsilon + \epsilon_p$ . It remains to add the Fermi energy  $\mu_H$  of the single-band Hubbard model itself:

$$\mu = \epsilon_p + \epsilon + \mu_H$$

so that  $\mu - E_1 = \epsilon + \mu_H - 4t_{pp}$ . To evaluate  $\epsilon$  we use the parameter set given by Hybertsen *et al.*[46] in their Table I. The only exception is the direct oxygen-oxygen hopping. Here we use the value  $t_{pp} = 0.37eV$  which has been extracted directly from experiment in Ref. [42] where it also was found to be consistent with previous estimates. We then obtain  $\epsilon = 1.82 eV$ . The Fermi energy of the single-band Hubbard model may be estimated from exact diagonalization results. In a  $4 \times 4$  cluster this was found to be  $1.6 t$  at  $U/t = 8$ [47] and  $1.788 t$  at  $U/t = 10$ [48]. Hybertsen *et al.* estimated  $U = 5.4 eV$  and  $t = 0.43 eV$  so that  $U/t = 12.6$ . We estimate  $\mu_H \approx 2 t = 0.86 eV$  so that eventually  $\mu - E_1 = 1.2 eV$ . The value in Figure 1 of Meevasana *et al.* is  $\approx 1 eV$ . The agreement is reasonable given the uncertainty about some parameters but it is quite obvious that taking into account the binding energy  $\epsilon$  is indispensable to obtain a correct estimate of the Fermi energy.

The value of  $\mu - E_1$  obviously depends on  $t_{pp}$  so that small variations from one compound to the other may well explain the variations observed by Meevasana *et al.*. The Fermi energy of the Hubbard model will change with doping as well, but these changes are a fraction of  $J \approx 120 meV$ . Accordingly, the distance between the free-electron-like state at  $\Gamma$  and the Fermi energy should always be  $\approx 1 eV$  and this is indeed the case in Bi2201 and Bi2212[8]. All in all one can say that the consequent application of the ZRS picture can explain the position of the Fermi energy relative to a 1eV peak - which forms a natural intrinsic reference energy - quite well.

## V. SUMMARY AND DISCUSSION

In summary, we have investigated the relationship between the single-particle spectra of actual charge-transfer models and corresponding 'effective' single band Hubbard models. In the noninteracting case  $U = 0$  the charge transfer models have several bands and it was found that those bands with predominant ligand (i.e.  $p$  character in the present models) are almost unaffected by the strong correlations. Bands with predominant  $d$ -character are split into two Hubbard bands which can be mapped quite well to those of an effective single-band Hubbard model. It turned out that the spectra of  $p$  and  $d$  electrons to good approximation can be obtained from that of the single band Hubbard model by a constant shift in energy - the binding energy of the Zhang-Rice singlet - and, in the case of the  $p$ -like spectrum, by a factor which might be termed the form factor of the Zhang-Rice singlet.

These results give a natural explanation for the waterfall phenomenon in terms of a pure matrix element effect - as has previously been inferred by Inosov *et al.*[7, 10] and Zhang *et al.*[13] from an analysis of their experimental data. Here one has to distinguish between two different effects: the first one - pointed out already by Ronning *et al.*[1] - applies only to the special situation of near-normal emission of photoelectrons. Here the vanishing of the dipole matrix element  $\langle f | \mathbf{A} \cdot \mathbf{p} | i \rangle$  makes it impossible to observe ZRS-derived states.

The second matrix element effect is the form factor of the Zhang-Rice singlet mentioned above, which describes the interference between the phases of the  $p$ -like photohole and those of the O2p-orbitals 'within' a Zhang-Rice singlet - which locally correspond to a state with momentum  $(\pi, \pi)$ . This makes it impossible to couple to a ZRS-derived state by creating a  $p$ -like photohole with momenta near  $(2n\pi, 2m\pi)$  with integer  $n$  and  $m$ .

These two simple rules explain under which experimental conditions the waterfall is observed or not: in the hole-doped compounds and at photon energies where predominantly O2p-like holes are produced, the quasiparticle band around  $\Gamma$  can be observed neither in the first nor in any higher Brillouin zone and instead the waterfall appears. If photon energies where Cu3d holes are generated are used, the quasiparticle band cannot be observed in the first BZ, but in higher Brillouin zones. In this case the waterfall is absent and no kink in the quasiparticle band appears.

In the electron-doped compounds the quasiparticles correspond to extra electrons in Cu3d <sub>$x^2-y^2$</sub>  orbitals so that the considerations regarding the form factor of the ZRS do not apply. The argument regarding the vanishing of the dipole matrix element  $\langle f | \mathbf{A} \cdot \mathbf{p} | i \rangle$ , however, remain unchanged so that the quasiparticle band around  $\Gamma$  cannot be observed in the first Brillouin zone either - this has indeed been observed by Ikeda *et al.*[11] and Moritz *et al.*[12]. It should be possible, however, to observe the full quasiparticle band without a kink in a higher Brillouin zone.

In those cases where the 'dark region' around  $\Gamma$  is present, the apparent vertical part of the waterfall corresponds to the incoherent continua in the single-particle spectral function of the t-J model. Since these continua are formed from states which also correspond to Zhang-Rice singlets, they become extinct near  $(2n\pi, 2m\pi)$  as well. Additional evidence comes from the fact that these band portions show the same dependence on photon polarization as the quasiparticle band itself[5].

Finally, the high intensity bands observed at  $\Gamma$  at binding energies higher than  $\approx 1 eV$  have no correspondence in a single-band Hubbard or t-J model - otherwise they would not be observed in normal emission - but are precisely the bands of predominant O2p-character which remain unaffected by the strong correlations. They are analogous to the 1eV-peaks observed at high-symmetry points in cuprates[42] and correspond to O2p driven states which have little or no hybridization with the strongly corre-

lated  $d$ -orbitals. These states therefore are essentially single particle states, which immediately explains their much higher intensity as compared to the quasiparticle band.

All in all the present theory indicates that the waterfall phenomenon constitutes an experimental proof of the Zhang-Rice construction of a single-band Hubbard or  $t$ - $J$  model to describe the low energy states of the  $\text{CuO}_2$  planes and in fact provides a direct visualization of the energy range in which the states of the real  $\text{CuO}_2$ -plane correspond to those of a single-band Hubbard or  $t$ - $J$  model. It shows moreover that the incoherent continua predicted by various calculations for the  $t$ - $J$  or Hubbard model are indeed observable in experiment in that

they are responsible for the vertical part of the waterfalls themselves.

Acknowledgement: K. S. acknowledges the JSPS Research Fellowships for Young Scientists. R. E. most gratefully acknowledges the kind hospitality at the Center for Frontier Science, Chiba University. This work was supported in part by a Grant-in-Aid for Scientific Research (Grant No. 22540363) From the Ministry of Education, Culture, Sports, Science and Technology of Japan. A part of the computations was carried out at the Research Center for Computational Science, Okazaki Research Facilities and the Institute for Solid State Physics, University of Tokyo.

- 
- [1] F. Ronning, K. M. Shen, N. P. Armitage, A. Damascelli, D. H. Lu, Z. X. Shen, L. L. Miller, and C. Kim, *Phys. Rev. B* **71**, 094518 (2005).
- [2] J. Graf, G.-H. Gweon, K. McElroy, S.Y. Zhou, C. Jozwiak, E. Rotenberg, A. Bill, T. Sasagawa, H. Eisaki, S. Uchida, H. Takagi, D.-H. Lee, and A. Lanzara, *Phys. Rev. Lett.* **98**, 067004 (2007).
- [3] B. P. Xie, K. Yang, D. W. Shen, J. F. Zhao, H. W. Ou, J. Wei, S. Y. Gu, M. Arita, S. Qiao, H. Namatame, M. Taniguchi, N. Kaneko, H. Eisaki, K. D. Tsuei, C. M. Cheng, I. Vobornik, J. Fujii, G. Rossi, Z. Q. Yang, and D. L. Feng, *Phys. Rev. Lett.* **98**, 147001 (2007).
- [4] T. Valla, T. E. Kidd, W.-G. Yin, G. D. Gu, P. D. Johnson, Z.-H. Pan, and A. V. Fedorov, *Phys. Rev. Lett.* **98**, 167003 (2007).
- [5] Z.-H. Pan, P. Richard, A.V. Fedorov, T. Kondo, T. Takeuchi, S.L. Li, Pengcheng Dai, G.D. Gu, W. Ku, Z. Wang, and H. Ding, *arXiv:cond-mat/0610442* (2006).
- [6] J. Chang, S. Pailhes, M. Shi, M. Manson, T. Claesson, O. Tjernberg, J. Voigt, V. Perez, L. Patthey, N. Momono, M. Oda, M. Ido, A. Schnyder, C. Mudry, and J. Mesot, *Phys. Rev. B* **75**, 224508 (2007).
- [7] D. S. Inosov, J. Fink, A. A. Kordyuk, S. V. Borisenko, V. B. Zabolotnyy, R. Schuster, M. Knupfer, B. Buechner, R. Follath, H. A. Duerr, W. Eberhardt, V. Hinkov, B. Keimer, and H. Berger, *Phys. Rev. Lett.* **99**, 237002 (2007).
- [8] W. Meevasana, X. J. Zhou, S. Sahrakorpi, W. S. Lee, W. L. Yang, K. Tanaka, N. Mannella, T. Yoshida, D. H. Lu, Y. L. Chen, R. H. He, Hsin Lin, S. Komiya, Y. Ando, F. Zhou, W. X. Ti, J. W. Xiong, Z. X. Zhao, T. Sasagawa, T. Kakeshita, K. Fujita, S. Uchida, H. Eisaki, A. Fujimori, Z. Hussain, R. S. Markiewicz, A. Bansil, N. Nagaosa, J. Zaanen, T. P. Devereaux, and Z.-X. Shen, *Phys. Rev. B* **75**, 174506 (2007).
- [9] W. Meevasana, F. Baumberger, K. Tanaka, F. Schmitt, W. R. Dunkel, D. H. Lu, S. K. Mo, H. Eisaki, and Z. X. Shen, *Phys. Rev. B* **77**, 104506 (2008).
- [10] D. S. Inosov, R. Schuster, A. A. Kordyuk, J. Fink, S. V. Borisenko, V. B. Zabolotnyy, D. V. Evtushinsky, M. Knupfer, B. Bchner, R. Follath, and H. Berger, *Phys. Rev. B* **77**, 212504 (2008); **79**, 139901(E) (2009).
- [11] M. Ikeda, T. Yoshida, A. Fujimori, M. Kubota, K. Ono, Y. Kaga, T. Sasagawa, and H. Takagi *Phys. Rev. B* **80**, 184506 (2009).
- [12] B. Moritz, F. Schmitt, W. Meevasana, S. Johnston, E. M. Motoyama, M. Greven, D. H. Lu, C. Kim, R. T. Scalettar, Z.-X. Shen, *New Journal of Physics* **11**, 093020 (2009).
- [13] W. Zhang, G. Liu, J. Meng, L. Zhao, H. Liu, X. Dong, W. Lu, J. S. Wen, Z. J. Xu, G. D. Gu, T. Sasagawa, G. Wang, Y. Zhu, H. Zhang, Y. Zhou, X. Wang, Z. Zhao, C. Chen, Z. Xu, and X. J. Zhou, *Phys. Rev. Lett.* **101** (2008) 017002.
- [14] D. E. Eastman and J. L. Freeouf, *Phys. Rev. Lett.* **34**, 395 (1975).
- [15] B. O. Wells, Z.-X. Shen, A. Matsuura, D. M. King, M. A. Kastner, M. Greven, and R. J. Birgeneau, *Phys. Rev. Lett.* **74**, 964 (1995).
- [16] F. Ronning, C. Kim, D. L. Feng, D. S. Marshall, A. G. Loeser, L. L. Miller, J. N. Eckstein, L. Bozovic, and Z.-X. Shen, *Science* **282**, 2067 (1998).
- [17] B. Kyung and R. A. Ferrell, *Phys. Rev. B* **54**, 10125 (1996).
- [18] F. Lema, and A. A. Aligia, *Phys. Rev. B* **55**, 14092 (1997)
- [19] A. L. Chernyshev, A. V. Dotsenko, and O. P. Sushkov, *Phys. Rev. B* **49**, 6197 (1994).
- [20] V. I. Belinicher, A. L. Chernyshev, A. V. Dotsenko, and O. P. Sushkov, *Phys. Rev. B* **51**, 6076 (1995).
- [21] J. Baa, A. M. Ole, and J. Zaanen, *Phys. Rev. B* **52**, 4597 (1995).
- [22] N. M. Plakida, V. S. Oudovenko, P. Horsch, and A. I. Liechtenstein, *Phys. Rev. B* **55**, R11997 (1997).
- [23] V. I. Belinicher, A. L. Chernyshev, and V. A. Shubin, *Phys. Rev. B* **56**, 3381 (1997).
- [24] O. P. Sushkov, G. A. Sawatzky, R. Eder, and H. Eskes, *Phys. Rev. B* **56**, 11769 (1997).
- [25] K. J. von Szczepanski, P. Horsch, W. Stephan and M. Ziegler, *Phys. Rev. B* **41**, 2017 (1990).
- [26] E. Dagotto, R. Joynt, A. Moreo, S. Bacci and E. Gagliano, *Phys. Rev. B* **41**, 9049 (1990).
- [27] P. W. Leung and R. J. Gooding *Phys. Rev. B* **52**, R15711 (1995).
- [28] P. W. Leung, B. O. Wells, and R. J. Gooding *Phys. Rev. B* **56**, 6320 (1997).
- [29] C. Kim, Z.-X. Shen N. Motoyama, H. Eisaki, S. Uchida, T. Tohyama, and S. Maekawa *Phys. Rev. B* **56**, 15589, (1997).

- [30] A. Koitzsch, S. V. Borisenko, J. Geck, V. B. Zabolotnyy, M. Knupfer, J. Fink, P. Ribeiro, B. Behner, and R. Follath Phys. Rev. B **73**, 201101 (2006).
- [31] S. Basak, T. Das, H. Lin, J. Nieminen, M. Lindroos, R. S. Markiewicz, and A. Bansil, Phys. Rev. B **80**, 214520 (2009).
- [32] A. Bansil and M. Lindroos, Phys. Rev. Lett. **83**, 5154 (1999).
- [33] M. Lindroos, S. Sahrakorpi, and A. Bansil, Phys. Rev. B **65**, 054514 (2002).
- [34] S.-J. Oh, J. W. Allen, I. Lindau, and J. C. Mikkelsen, Jr., Phys. Rev. B **26**, 4845 (1982).
- [35] A. Macridin, M. Jarrell, T. Maier, and D. J. Scalapino, Phys. Rev. Lett. **99**, 237001 (2007).
- [36] M. M. Zemljic, P. Prelovsek, and T. Tohyama Phys. Rev. Lett. **100**, 036402 (2008).
- [37] B. Moritz, S. Johnston, and T. P. Devereaux, preprint arXiv:1004.4685.
- [38] C. Gröber, R. Eder, and W. Hanke, Phys. Rev. B **62**, 4336 (2000).
- [39] P. J. Feibelman and D. E. Eastman, Phys. Rev. B **10**, 4932 (1974).
- [40] F. C. Zhang and T. M. Rice, Phys. Rev. B **37**, 3759 (1988).
- [41] Z. X. Shen *et al.*, Phys. Rev. B **44**, 3604 (1991).
- [42] J. J. Pothuizen, R. Eder, N. T. Hien, M. Matoba, A. A. Menovsky, and G. A. Sawatzky, Phys. Rev. Lett. **78**, 717 (1997). Phys. Rev. B **41**, 9049 (1990).
- [43] R. Eder and Y. Ohta, Phys. Rev. B **56**, 2542 (1997).
- [44] S. Schmitt Rink, C. M. Varma and A. E. Ruckenstein, Phys. Rev. Lett. **60**, 2793 (1988).
- [45] G. Martinez and P. Horsch, Phys. Rev. B **44**, 317 (1991)
- [46] M. S. Hybertsen, E. B. Stechel, M. Schlter and D. R. Jennison, Phys. Rev. B **41**, 11 068 (1990).
- [47] E. Dagotto, F. Ortolani, and D. Scalapino, Phys. Rev. B **46**, 3183 (1992).
- [48] P. W. Leung, Z. Liu, E. Manousakis, M. A. Novotny, and P. E. Oppenheimer, Phys. Rev. B **46**, 11779 (1992).
- [49] M. Potthoff, Eur. Phys. J. B **36**, 335 (2003)
- [50] M. Potthoff, Eur. Phys. J. B **32**, 429 (2003).
- [51] J. M. Luttinger and J. C. Ward, Phys. Rev. **118**, 1417 (1960).
- [52] D. Senechal, arXiv:00806.2690.
- [53] E. Arrigoni, M. Aichhorn, M. Daghofer, and W. Hanke, New. J. Phys. **11**, 055066 (2009).
- [54] P. Wróbel, W. Suleja, and R. Eder Phys. Rev. B **78**, 064501 (2008).
- [55] D. Senechal, D. Perez, and M. Pioro-Ladriere, Phys. Rev. Lett. **84**, 522 (2000).
- [56] D. Senechal, D. Perez, and D. Plouffe, Phys. Rev. B **66**, 075129 (2002).